Dalton Transactions

Accepted Manuscript

ROYAL SOCIETY OF CHEMISTRY

www.rsc.org/dalton

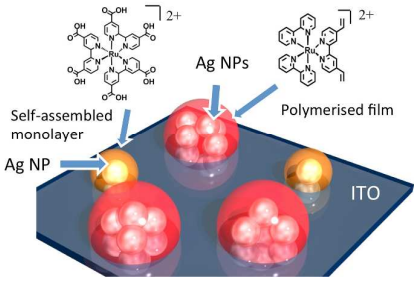

Two types of hybrid films of AgNPs and ruthenium complexes are constructed via chemical bond formation and electro reductive polymerization.

Journal Name

RSCPublishing

ARTICLE

Construction of hybrid films of silver nanoparticles and polypyridine ruthenium complexes on substrates

Cite this: DOI: 10.1039/x0xx00000x

Received 00th January 2012,
Accepted 00th January 2012

DOI: 10.1039/x0xx00000x

www.rsc.org/

Azusa Kajikawa,[a] Takanari Togashi,[a] Yuka Orikasa,[a] Bin Bin Cui,[b] Yu-Wu Zhong,[b] Masatomi Sakamoto,[a] Masato Kurihara,*[a] Katsuhiko Kanaizuka*[a]

Hybrid films of functional molecules and metal nanoparticles have been considered to be novel photo-functional devices. Here we have successfully constructed hybrid films of silver nanoparticles and ruthenium polypyridine derivatives on substrates. In order to hybridise them on a surface, a self-assembled monolayer method via chemical bond formation and electro-reductive polymerisation (thick layers) via physical attachment have been employed. These methods have the advantage of convenient and reproductive fabrications of complicated hybrid films. Furthermore, it has been clarified that these hybrid films show unique photo-functional behaviours, such as enhanced photocurrent generation.

1. Introduction

Polypyridine ruthenium complexes (RuL_n) are well-known as useful photosensitisers because of their long lifetime of excited state upon light absorption, redox activity of Ru(III/II) and polypyridine ligands, and thermodynamical stability.[1] Therefore, these complexes have been used to construct DSSCs,[2] solid-state electro-generated chemiluminescence (ECL),[3] and oxygen sensors.[4] In order to enhance the functions of these devices, the construction of hybrid films of RuL_n and other materials, such as metal nanoparticles (NPs), [5] is important. However, there are few reports on convenient construction of hybrid films to date.

We have considered that one of the effective ways to obtain enhanced photocurrent systems is the employment of metal NPs[6] because of their unique localised surface plasmon resonance (LSPR) behaviour upon light irradiation.[7] Specifically, the LSPR of silver NPs (Ag NPs) appears around 400 nm, and this LSPR couples interact with each other under high concentration on a substrate; this LSPR couple is called a gap-mode plasmon, and these bands appear between 400 and 550 nm.[8] This gap-mode plasmon band can overlap with the metal-to-ligand charge transfer (MLCT) of RuL_n; therefore, it has the ability to enhance photocurrent efficiency by the combination of RuL_n and Ag NPs on an electrode.[9]

We have employed two types of ruthenium complexes in this study, described in Figure 1(a). One complex has three simple 2,2'-bipyridine ligands bearing two carboxyl groups (4,4'-dicarboxy-2,2'-bipyridine: dcbpy), **1**.[10] This complex is used for Grätzel-type dye-sensitised solar cells. Carboxyl group can attach not only to a metal oxide surface,[11] such as TiO_2, but also to a soft metal NP surface, such as Ag.[8a] This complex fixation technique on a substrate via chemical bond formation, developed by Ulman, is called a self-assembled monolayer (SAM).[12] Meyer and co-workers report on the construction of an efficient and rapid excited-state electron injection system

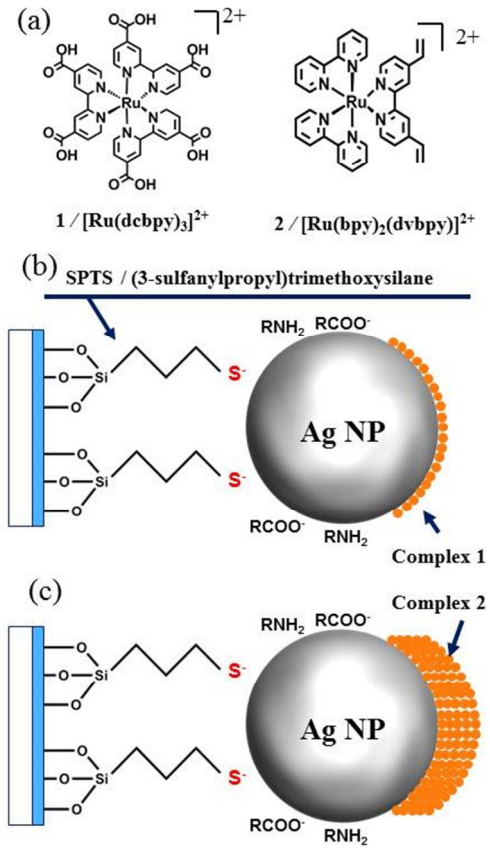

Fig. 1 Chemical structure of ruthenium complexes used in this study (a) and images of surface hybrid films of substrate/SPTS/Ag NP/**1** (b) and substrate /SPTS/Ag NP/**2** (c).

using this system.[13] The combination system of Ru(II)(dcbpy)$_3$ complex (**1**) and Ag NP on ITO (indium-tin oxide) is shown in Figure 1(b).

Another complex used in this study has two 2,2'-bipyridine (bpy) ligands and one bpy ligand bearing two vinyl groups (dvbpy), **2**.[14] This type of complex is fixed on an electrode by not oxidative but reductive electropolymerisation. Employing this method, oxidation of Ag NPs can be protected. This electropolymerisation was developed by Abruna and Murray.[15] The film thickness of the complex can be controlled by the reduction time, and rectification behaviour in bilayer systems can also be constructed. Recently, the construction of a composite system of an electropolymerised iron(II) complex and fluorine-doped tin oxide (FTO) NPs and its catalytic application was reported by Meyer.[16] The combination system of ruthenium(II) complex (**2**) and Ag NP on ITO is shown in Figure 1(c).

Here we report on the convenient construction of two types of surface hybrid films of Ag NPs and polypyridine ruthenium complexes on substrates. We have clarified that an enhanced photocurrent generating system can be prepared.

2. Experimental

2.1 Materials

Acetonitrile (CH_3CN), chloroform ($CHCl_3$), methanol (CH_3OH), and 2-propanol were purchased from Kanto Chemicals. 3-Sulfanylpropyltrimethoxysilane (SPTS) was purchased from TCI. An ink of Ag NPs in organic solvent was prepared by a method similar to that in a previous paper.[8a] Compounds **1** and **2** were synthesised according to the previous paper.[10,14] ITO (10 ohms/cm^2, GEOMATEC Co., Ltd.) substrates were washed with 2-propanol, methanol, and then pure water before use. Tetra-*n*-butylammonium perchlorate (TBAP) and Na_2SO_4 were purchased from Nacalai Tesque. $TBAPF_6$ was purchased from TCI and used after recrystallisation from ethanol.

2.2 Methods

Cyclic voltammetry was carried out using ALS electrochemical analyser model 660A in 0.1 M Na_2SO_4 aqueous solution or 0.1 M TBAP CH_3CN solution. For electrochemical polymerisation of the ruthenium complex, an electrolyte solution was degassed with argon bubbling for 10 min. Atomic force microscope (AFM) images were observed using Shimadzu SPM-9600. UV-vis absorption spectra were monitored using Shimadzu UV-3150. Cross-section field emission scanning electron microscope (FE-SEM) measurement was carried out using JSM-7600F. A dip coater (Asumi Giken N100) was used for the fixation of Ag NPs on a substrate.

2.3 Preparation of ITO/SPTS/Ag NPs and ITO/Ag NPs

In the first step, we formed a self-assembled monolayer (SAM) using 3-sulfanylpropyltrimethoxysilane (SPTS) on an ITO electrode or glass plate. An ITO electrode or glass was immersed in a 20 mM methanol solution of SPTS for 3 hrs at 50^{o}C, and after rinsing with methanol, an ITO/SPTS substrate was obtained. Ag NPs were fixed on the ITO/SPTS substrate in the second step: the ITO/SPTS electrode was immersed in a dispersion solution of Ag NPs (10 mg in 12 mL of a mixture of butanol and octane (1:4 v/v); the mean particle size is 11 ± 1.9 nm, estimated from an SEM image) and slowly pulled up at a speed of 0.3 mm/s using a dip coater. The physically attached Ag NPs were carefully removed from the modified ITO electrode with octane. Thus an ITO/SPTS/Ag NP film was prepared.[8a] In order to prepare ITO/Ag NPs without SPTS, ITO was directly immersed in a dispersion solution of Ag NPs and then physically fixed using the dip coater described above.

2.4 Hybrid film of 1 on ITO/SPTS/Ag NPs

ITO/SPTS/Ag NPs/**1** substrate was prepared as follows: **1** was embedded on the ITO/SPTS/Ag NP electrode by its simple immersion into a CH_3CN solution of **1** (0.1 mM) for 30 min at room temperature. The resulting hybrid film was thoroughly washed with a CH_3CN solvent and dried under a stream of nitrogen gas.

2.5 Hybrid film of 2 on ITO/SPTS/Ag NPs

An ITO/SPTS/Ag NP electrode and two electrodes (a Pt counter electrode and a Ag/Ag$^+$ reference electrode) were immersed in a 0.1 M TBAP CH_3CN solution containing 0.5 mM ruthenium complex **2** under Ar. The negative bias was applied to the ITO electrode (vs. Ag/Ag$^+$ reference electrode) for various periods of time at room temperature.

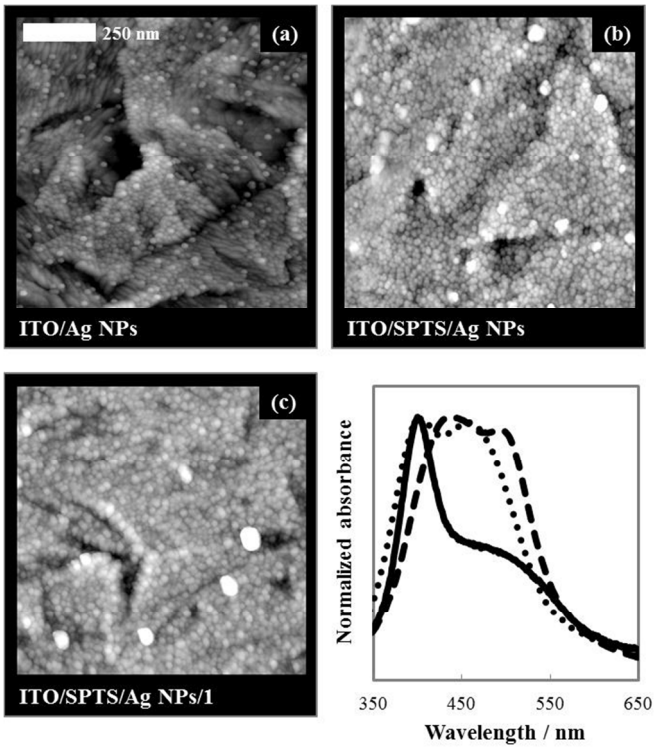

Fig. 2 AFM images of ITO/Ag NPs (a), ITO/SPTS/Ag NPs (b), and ITO/SPTS/Ag NPs/**1** (c). Normalised electronic spectra of ITO/Ag NPs (solid), ITO/SPTS/Ag NPs (dot), and ITO/SPTS/Ag NPs/**1** (dash).

2.6 Photocurrent responses of hybrid films of ITO/SPTS/Ag NPs/1

The photocurrent generation behaviour of ITO/SPTS/Ag NPs/**1** was tested in a 0.1 M $TBAPF_6$ $CHCl_3$ with or without oxygen by Ar bubbling.

3. Results and discussion

3.1 AFM images and UV-vis absorption spectra of ITO/Ag NPs, ITO/SPTS/Ag NPs, and ITO/SPTS/Ag NPs/1

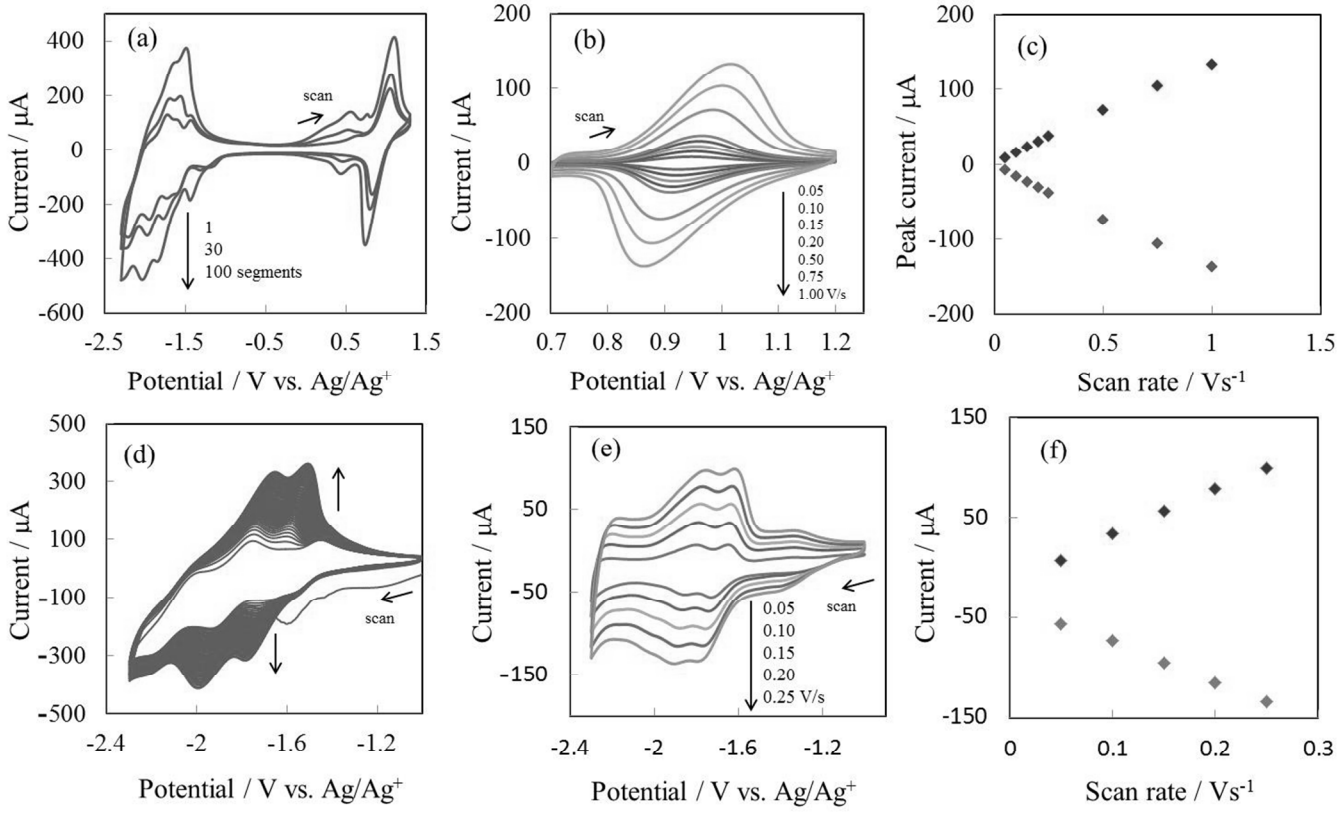

Fig. 3 CVs (1, 30, and 100 segments) of **2** (0.5 mM) at ITO at 0.1 V/s in 0.1 M TBAP CH_3CN (a); CVs of ITO/**2** in 0.1 M TBAP CH_3CN at various scan rates (b); plots of peak anodic and cathodic currents of a Ru(III/II) couple in Figure 3b (c); CVs of 2 (0.5 mM) at ITO/SPTS/Ag NPs electrode (from 1 to 50 segments) (d); CVs of ITO/SPTS/Ag NPs/**2** in 0.1 M TBAP CH_3CN at various scan rates (e); and plots of peak anodic and cathodic currents of the reduction wave in Figure 3e (f).

AFM images of ITO/Ag NPs, ITO/SPTS/Ag NPs, and ITO/SPTS/Ag NPs/**1** are shown in Figure 2a–c. The brighter dots are ascribable to Ag NPs fixed on the ITO electrodes. In the case of ITO/Ag NPs, large areas of the bare ITO surface are exposed. In contrast, by using SPTS as an anchoring molecule, the ITO/SPTS surface was almost completely covered by Ag NPs and formed a homogeneous layer (Figure 2b). No significant elimination of the densely covered Ag NPs occurred from the ITO/SPTS substrate by ultrasonic irradiation. A plausible mechanism to generate such a stable Ag NP-attached layer was chemical bond formation, which has been previously reported.[8a] The homogeneous Ag NP layer was kept after the immersion in the CH_3CN solution of **1** (Figure 2c).

The normalised UV-vis absorption spectra of ITO/Ag NPs, ITO/SPTS/Ag NPs, and ITO/SPTS/Ag NPs/**1** are shown in Figure 2d. The normalised absorption maximum at λ_{max} = 400 nm is assigned to the normal plasmon band of individually isolated Ag NPs (solid line in Figure 2d).[8a] The plasmonic gap-mode absorption was observed at λ_{max} = 466 nm, which appeared in limited nano-gaps among closely located Ag NPs as the secondary enhanced plasmonic interaction between Ag NPs (dotted line in Figure 2d). A red shift in the absorption bands is observed after immersion in a solution of **1**, probably because of electronic communication between Ag NPs and **1** or the location (distance) of Ag NPs is changed,[17] and the absorption of complex **1** (MLCT band) is included. These results indicate that stepwise fabrication of metal NPs and functional molecules can be carried out using the convenient dipping method.

3.2 Electrochemical deposition of 2 on ITO and ITO/SPTS/Ag NPs

Figure 3a shows cyclic voltammograms of **2** (0.5 mM) at ITO (vs. Ag/Ag^+) in 0.1 M TBAP CH_3CN solution. In the first scan, a reversible one-electron oxidation wave based on Ru(III/II) at 0.98 V and four reduction waves at -1.50, -1.81, -2.06, and -2.27 V were observed, which is based on a vinyl group and bpy.[14] The peak current was increased with the increase of the scan number; this behaviour has been already reported.[14] This indicates that the stepwise polymerisation of vinyl groups between Ru complexes occurred at the ITO surface. In the large number of segments (ca. 100 segments), a charge-trapping effect, that is a limited electron transfer in thicker film, was clearly observed before the oxidation potential of the Ru (III/II) couple and the reduction potential of the ligand. This result supports the formation of layered film on the electrode.[13,14] Figure 3b shows plots of peak anodic and cathodic currents of the Ru(III/II) wave of ITO/**2** in 0.1 M TBAP CH_3CN solution. The peak currents were linearly increased with the scan rates, indicative of surface combined species.

The reversible waves of **2** were not observed when the ITO/SPTS/Ag NP electrode was used under the same conditions. This probably indicates that oxidation of Ag NPs occurs at 0.2 V (vs. Ag/Ag^+), and decomposition of film occurs at a positive region. One of the advantages of complex **2** is reductive polymerisation behaviour. Therefore, we monitored the polymerisation behaviour of **2** on the ITO/SPTS/Ag NP electrode in the negative region. Cyclic voltammograms of **2**

(0.5 mM) on ITO/SPTS/Ag NPs in the negative region are shown in Figure 3c. An increase in currents was observed upon the application of voltage, which indicated that stepwise molecular fabrication occurred on the ITO/SPTS/Ag NPs surface.

3.3 AFM and SEM images of ITO/SPTS/Ag NPs/2 and ITO/2

An AFM image of ITO/SPTS/Ag NPs/**2** is shown in Figure 4a. After the polymerisation of complex **2** on ITO/SPTS/Ag NPs, brighter dots of the size 80–140 nm were observed at the surface, which were not observed before polymerisation. We consider that these large dots are Ag NPs aggregated upon voltage application, because the Ag NP surfaces are covered with an aliphatic chain by weak coordination.

This aggregation behaviour was also monitored by cross-section FE-SEM images ITO/SPTS/Ag NPs/**2**, as shown in Figure 4b. This cross-section FE-SEM image is largely difference from that of ITO/**2** (25 segments, see Figure 4c), and the uniform film of **2** was formed on ITO electrode. The thickness of film was increased with the increase of segment number.

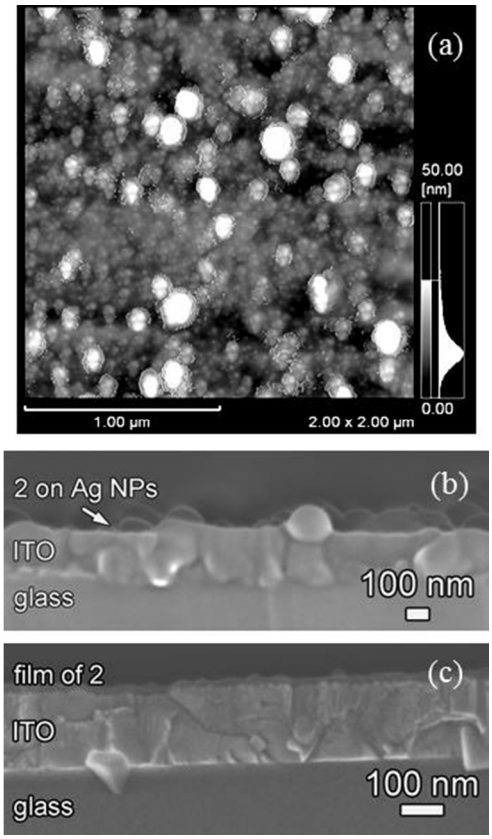

Fig. 4. (a) AFM image of ITO/SPTS/Ag NPs/**2** (100 segments) and cross-section FE-SEM images of (b) ITO/SPTS/Ag NPs/**2** (100 segments) and (c) ITO/**2** (25 segments).

3.4 Photocurrent generation behaviour of hybrid film of 1

In order to consider the merit of a composite system, that is, the effect of Ag NPs, we measured photocurrents. The photocurrent generation behaviour of ITO/**1**, ITO/SPTS, ITO/SPTS/Ag NPs, and ITO/SPTS/Ag NPs/**1** was investigated in a 0.1 M $TBAPF_6$ $CHCl_3$ solution at -0.5 V (vs. Ag/Ag^+). In

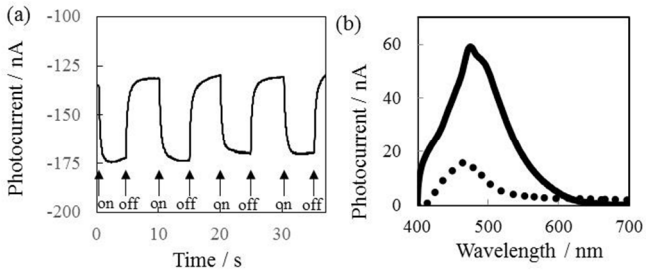

Fig. 5. (a) Photocurrent responses of ITO/SPTS/Ag NPs/**1** at 456 nm and (b) photocurrent dependence on wavelength of ITO/**1** (dot) and ITO/SPTS/Ag NPs/**1** (solid line) in 0.1 M $TBAPF_6$ $CHCl_3$ at -0.5 V vs. Ag/Ag^+.

the cases of ITO/**1** and ITO/SPTS/Ag NPs/**1** systems, the stable cathodic photocurrents were observed upon light irradiation at 456 nm (see Figure 5). We consider that complex **1** and Ag Np on the ITO was protected by long alkyl amines. The action spectrum of ITO/**1** as shown in Figure 5 is nicely fitted to the absorption spectrum (MLCT), suggesting that the photo-excitation states of **1** act as the exclusive trigger on ITO (no photocurrent is observed for ITO/Ag NPs or ITO/SPTS/Ag NPs).[18] It is important that the action spectra of ITO/SPTS/Ag NPs/**1** are significantly different from the absorption spectra; the photocurrent was strongly enhanced between 530 and 600 nm. This is probably caused by the effect of the mode-gap plasmonic interaction of the densely arranged Ag NPs with **1**.

The plausible mechanism of photocurrent generation is considered as follows: (1) photo-excitation of **1** triggered the initial electron transfer in the photocurrent generation, and (2) electron and/or energy transfer from the photo-excited **1** to oxygen molecules dissolved in the solution took place, and at the same time, (3) electron injection from Ag NPs to the photochemically oxidised **1** occurred. As a result, a cathodic photocurrent was observed. Thus, the enhanced and effective electron-transfer system upon light irradiation can be constructed by the hybridisation of $Ru(II)bpy_3$ complex film and Ag NPs on a substrate.

3.5 Photocurrent generation behaviour of hybrid film of 2

Photocurrent generation behaviour of ITO/**2** and ITO/SPTS/Ag NPs/**2** was also investigated in the similar conditions of complex **1**. Figure 6 shows photocurrent responses upon light irradiation at 456 nm at -0.2 V vs. Ag/Ag^+. The value of photocurrent in ITO/SPTS/Ag NPs/**2** (ca. 5 nA) was slightly larger than that in ITO/**2** (ca.2 nA) indicating of effective electron transfer occurred by the hybridisation of Ag NPs on

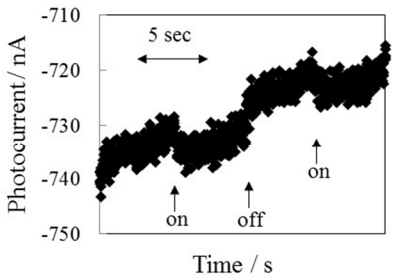

Fig. 6. Photocurrent responses of ITO/SPTS/Ag NPs/**2** at 456 nm in 0.1 M $TBAPF_6$ $CHCl_3$ at -0.2 V vs. Ag/Ag^+.

ITO. Unfortunately we have not clarified the effect of the mode-gap plasmonic interaction for the photocurrent generation because of the action spectrum was not well obtained in this case. We consider that (1) thickness of **2** on Ag NP depends on the rate of electron transfer[20] and/or (2) aggressive oxygen molecules that is formed by the reduced oxygen attack to the uncovered complex **2** on ITO.

Conclusions

We have successfully constructed two types of ruthenium complex hybrid films on a Ag NP-modified electrode by convenient approaches. A self-assembled monolayer method via chemical bond formation produces reproductive fabrications of complicated hybrid films without damage to the delicate surface. Another method is an electro-reductive polymerisation system via physical attachment, which produces a thicker molecular film within a short period of time. However, this method causes some damage to the films by the voltage application. We consider this problem to be soluble by the employment of stable metal NP inks, that is, the surface of NPs covered with alkylthiols or rigid molecules. Additionally, we have clarified that these films show enhanced photocurrent generation upon light irradiation. These combined systems of functional metal complexes and metal NPs can open the field of smart photo-responsive and catalytic devices.[19]

Acknowledgements

This work was supported by a KAKENHI (No. 25810033) Grant-in-Aid for Young Scientists and by the Ministry of Education, Science, and Sports-Japan. This work was also partially supported by Dissemination of Tenure Tracking System Program of Ministry of Education, Culture, Sports, Science and Technology-Japan.

Notes and references

[a] Department of Material and Biological Chemistry, Faculty of Science, Yamagata University, 1-4-12 Kojirakawa-machi, Yamagata 990-8560, Japan
E-mail: kanaizuka@sci.kj.yamagata-u.ac.jp; Fax: +81-23-628-4856; Tel.: +81-23-628-4856
[b] Beijing National Laboratory for Molecular Sciences, CAS Key Laboratory of Photochemistry, Institute of Chemistry, Chinese Academy of Sciences, Beijing 100190, People's Republic of China

1 J.-P. Sauvage, J.-P. Collin, J.-C. Chambron, S. Guillerez and C. Coudret, *Chem. Rev.*, 1994, **94**, 993.
2 (a) B. O'Regan and M. Grätzel, *Nature*, 1991, **353**, 737. (b) M. Grätzel, *Nature*, 2001, **414**, 338.
3 (a) F. G. Gao and A. J. Bard, *J. Am. Chem. Soc.*, 2000, **122**, 7426. (b) K. M. Maness, R. H. Terrill, T. J. Meyer, R. W. Murray and R. M. Wightman, *J. Am. Chem. Soc.*, 1996, **118**, 10609.
4 K. Mori, M. Kawashima, M. Che and H. Yamashita, *Angew. Chem.*, 2010, **122**, 8780.
5 H. Goesmann, and C. Feldmann, *Angew. Chem. Int. Ed*., 2010, **49**, 1362.
6 (a) M. Itoh, T. Kakuta, M. Nagaoka, Y. Koyama, M. Sakamoto, S. Kawasaki, N. Umeda, and M. Kurihara, *J. Nanosci. Nanotechnol*., 2009, **9**, 6655. (b) X. Lu, M. Rycenga, S. E. Skabalak, B. Wiley and Y. Xia, *Annu. Rev*., 2009, **60**, 167. (c)
7 (a) M. Rycenga, C. M. Cobley, J. Zeng, W. Li, C. H. Moran, Q. Zhang, D. Qin and Y. Xia, *Chem. Rev.*, 2011, **111**, 3669. (b) D. V. Guzatov, S. V. Vaschenko, V. V. Stankevich, A. Y. Lunevich, Y. F. Glukhov and S. V. Gaponenko, *J. Phys. Chem. C,* 2012, **116**, 10723. (c) H. Nabika, M. Takase, F. Nagasawa and K. Murakoshi, *J. Phys. Chem. Lett.,* 2010, **1**, 2470. (d) K. Ikeda, K. Takahashi, T. Masuda and K. Uosaki, *Angew. Chem. Int. Ed.*, 2011, **50**, 1280.
8 (a) K. Kanaizuka, S. Yagyu, M. Ishizaki, H. Kon, T. Togashi, M. Sakamoto and M. Kurihara, *Appl. Phys. Lett.*, 2012, **101**, 063103.(b) A. L. Koh, K. Bao, I. Khan, W. E. Smith, G. Kothleitner, P. Nordlander, S. A. Maier and D. W. McComb, *ACS Nano*, 2009, **3**, 3015. (c) K. Kanaizuka, S. Yagyu, A. Kajikawa, T. Kakuta, H. Kon, T. Togashi, K. Uruma, M. Ishizaki, M. Sakamoto and M. Kurihara, *Chem. Lett*., 2013, **42**, 669. (d) T. Kakuta, H. Kon, A. Kajikawa, K. Kanaizuka, S. Yagyu, R. Miyake, M. Ishizaki, K. Uruma, T. Togashi, M. Sakamoto and M. Kurihara, *J. Nanosci. Nanotech*., 2014, **14**, 4090.
9 (a) C. Wen, K. Ishikawa, M. Kishima and K.Yamada, *Solar Energy Materials & Solar Cells*, 2000, **61**, 340-341. (b) S. D. Standridge, G. C. Schatz and J. T. Hupp, *J. Am. Chem. Soc*., 2009, **131**, 8407. (c) S. D. Standridge, G. C. Schatz and J. T. Hupp, *Langmuir*, 2009, **25**, 2596. (d) W.-J. Yoon, K.-Y. Jung, J. Liu, T. Duraisamy, R. Revur, F. L. Teixeira, S. Sengupta, and P. R. Berger, *Solar Energy Materials & Solar Cells*, 2010, **94**, 129. (e) R. Solarska, A. Krolokowska and J. Augustynski, *Angew. Chem. Int. Ed.*, 2010, **49**, 7983. (f) X. Chen, B. Jia, J. K. Saha, B. Cai, N. Stokes, Q. Qiao, Y. Wang, Z. Shi and M. Gu, *Nano Lett.*, 2012, **12**, 2187. (g) T. Arakawa, T. Munaoka, T. Akiyama and S. Yamada, *J. Phys. Chem. C*, 2009, **113**, 11830. (h) S. S. Kim, S. I. Na, J. Jo, D. Y. Kim and Y. C. Nah, *App. Phys. Lett.*, 2008, **93**, 073307.
10 K. Ocakoglu, E. Harputlu, P. Guloglu and S. Erten-Ela, *Inorganic Chemistry Communications*, 2012, **24**, 118-124.
11 (a) M. K. Nazeeruddin, A. Kay, I. Rodicio, R. H.-Baker, E. Müller, P. Liska, N. Vlachopoulos and M. Grätzel, *J. Am. Chem. Soc.,* 1993, **115**, 6382. (b) S. A. Trammell, J. A. Moss, J. C. Yang, B. M. Nakhla, C. A. Slate, F. Odobel, M. Sykora, B. W. Erickson and T. J. Meyer, *Inorg. Chem*, 1999, **38**, 3665. (c) D. Ma, S. E. Bettis, K. Hanson, M. Minakova, L. Alibabaei, W. Fondrie, D. M. Ryan, G. A. Papoian, T. J. Meyer, M. L. Waters and J. M. Papanikolas, *J. Am. Chem. Soc.,* 2013, **135**, 5250. (d) G. Will, G. Boschloo, S. N. Rao and D. Fitzmaurice, *J. Phys. Chem B*, 1999, **103**, 8067.
12 (a) A. Ulman, Chem. Rev., 1996, **96**, 1533. (b) H. Nishihara, *Chem. Lett.,* 2014, **43**, 388.
13 (a) E. Galoppini, W. Guo, W. Zhang, P. G. Hoertz, P. Qu and G. J. Meyer, *J. Am. Chem. Soc.,* 2002, **124**, 7801-7811. (b) G. Benkö, P. Myllyperkiö, J. Pan, A. P. Yartsev and V. Sundström, *J. Am. Chem. Soc.*, 2013, **125**, 1118. (c) H. D. Abruña, *Corrd. Chem. Rev*., 1988, **86**, 135.
14 H.–J. Nie, J.–Y. Shao, J. Wu, J. Yao and Y.–W. Zhong, *Organometallics*, 2012, **31**, 6952-6959.
15 (a) P. Denisevich, K. W. Willman, and R. W. Murray, *J. Am. Chem. Soc.,* 1981, **103**, 4727-4737. (b) K. Y. K. Man, H. L. Wong, W. K. Chan, *Langmuir*, 2006, **22**, 3368-3375. (c)

16 D. A. Torelli, D. P. Harrison, A. M. Lapides and T. J. Meyer, *ACS Appl Mater. Interfaces*, 2013, **5**, 7050-7057.

17 (a) L. Gunnarsson, T. Rindzevicius, J. Prikulis, B. Kasemo, M. Käll, S. Zou and G. C. Schatz, *J. Phys. Chem. B*, 2005, **109**, 1079. (b) F. Huang and J. Baumberg, *Nano Lett.*, 2010, **10**, 1787.

18 (a) K. Kanaizuka, S. Kato, H. Moriyama and C. Pac, *Res. Chem. Intermed*., 2007, **33**, 91. (b) P. K. Ghosh and T. G. Spiro, *J. Am. Chem. Soc.*, 1980, **102**, 5543. (c) A. Aoki, Y. Abe and T. Miyashita, *Langmuir*, 1999, **15**, 1463.

19 (a) T. Takahashi, A. Kudo, S. Kuwabata, A. Ishikawa, H. Ishihara, Y. Tsuboi and T. Torimoto, *J. Phys. Chem.C,* 2013, **117**, 2511. (b) F. Wang, C. Li, H. Chen, R. Jiang, L. -D. Sun, Q. Li, J. Wang, J. C. Yu and C. -H. Yan, *J. Am. Chem. Soc.*, 2013, **135**, 5588. (c) H. A. Atwater and A. Polman, *Nature Materials*, 2010, **9**, 205. (d) A. J. Morfa, K. L. Rowlen, T. H. Reilly, M. J. Romero and J. V. Lagemaat, *Appl. Phys. Lett.*, 2008, **92**, 013504.

20 (a) S. Creager, C. J. Yu, C. Bamdad, S. O'Connor, T. MacLean, E. Lam, Y. Chong, G. T. Olsen, J. Luo, M. Gozin, J. F. Kayyem, *J. Am. Chem. Soc.*, 1999, **121**, 1059. (b) Y. Matsu, K. Kanaizuka, K. Matsuo, Y.-W. Zhong, T. Nakae, E. Nakamura, *J. Am. Chem. Soc.*, 2008, **130**, 5016. (c) H. Nishihara, K. Kanaizuka, Y. Nishimori, Y. Yamanoi, *Coord. Chem. Rev*., 2007, **251**, 2674.

